

Enriching biologically relevant chemical space around 2-aminothiazole template for anticancer drug development

Sarah Titus¹ · Kumaran G. Sreejalekshmi¹

Received: 28 February 2017 / Accepted: 16 August 2017 / Published online: 28 August 2017
© Springer Science+Business Media, LLC 2017

Abstract Combinatorial library based on a biologically relevant core template, 2-aminothiazole, with immense scope of diversity multiplication was designed for anticancer therapeutics. The diversity elements were incorporated through azomethine linkage on C4 hydrazine terminus in 5-benzoyl-2-arylamino-1,3-thiazole using isopropyl, isobutyl, cyclohexyl, and benzyl fragments and enrichment of chemical space therein was evaluated. Molecular docking of an in-house 200-member virtual library in anticancer target proteins- estrogen receptor (3ERT), cyclin dependent kinase (3FDN), and Aurora kinase (3LAU), identified selective binding of the compounds as ATP competitive inhibitors of 3LAU. The synthetic access to the compounds was realized through a facile and economically viable [4 + 1] ring synthesis strategy employing commercially available reagents. The *in vitro* cytotoxicity of selected members against human cancer cell lines indicated the potential of the designed scaffold in anticancer drug discovery, where compounds **2b**, **3b**, and **4b** were found to be active against MCF-7 and A549 cell lines in less than ten micro molar concentrations. Moreover the predicted physicochemical properties pointed to the drug appropriateness for most of these molecules, that they obey the rule of five (RO5). Thus we present 2-alkyl/arylamino-4-alkylidene/arylidenehydrazino-5-benzoyl-1,3-thiazoles as a

prospective and expandable skeleton for diversity oriented synthesis and in the discovery of selective Aurora kinase inhibitors.

Keywords Chemical space · 2-Aminothiazole · HAT · VCHATL · Anticancer activity · Molecular docking

Introduction

The chemical space (Dobson 2004; Gorse 2006; Lipinski and Hopkins 2004) comprising small organic molecules is vast but largely unexplored whereas access to medicinally relevant chemical space with appropriate design and synthetic techniques is limited (Deng et al. 2013). Hence, the identification of novel small molecules within biological activity span is of utmost importance to chemical biology and drug discovery (Bennani 2012). Consequently, computer-based *de novo* drug design (Schneider and Schneider 2016; Rodrigues et al. 2015; Schneider and Fechner 2005) is currently re-emerging with a focus on generating innovative molecular scaffolds by accessing virtually infinite chemical space. Here, identification of novel drug-like small molecules with high structural diversity and quality are the prerequisite for new breakthroughs. The design of novel molecular libraries (Hajduk et al. 2011) can focus on (i) a relevant therapeutic target (John Harris et al. 2011; Sheppard and MacRitchie 2013; Prien 2005) or disease and (ii) the chemistry (Dimova and Bajorath 2016; Chen et al. 2005) or a desired molecular function. Despite the presence of numerous recurring molecular frameworks in bioactive molecules, the major challenge that still remains is the design of novel scaffolds

Electronic supplementary material The online version of this article (doi:10.1007/s00044-017-2039-y) contains supplementary material, which is available to authorized users.

✉ Kumaran G. Sreejalekshmi
sreeja@iist.ac.in

¹ Department of Chemistry, Indian Institute of Space Science and Technology, Valiamala Post-695 547, Thiruvananthapuram, India

capable to direct functional groups in a well-defined three dimensional (3D) space. The structural modification of compounds with established physiological or pharmacological effects for the production of novel and high quality lead molecules is an important aspect in medicinal chemistry and hence a key factor in drug development. In this context, heterocycles which can orient functional groups favorably are considered to be privileged structures and their presence in overall bioactive compound population gained them a significant position in modern drug development (Welsch et al. 2010; Dua et al. 2011; Song et al. 2014). Among heterocyclic ring systems, 1,3-thiazole has been the topic of interest for many researchers across the world because of its presence in many natural products and biomolecules and its wide spectrum of pharmacological activities. Biological importance of thiazoles varies from pharmacophoric and bioisosteric elements to spacers that made them suitable core in design and development of novel therapeutic agents (Ayati et al. 2015; Dilek Altıntop et al. 2016; Kashyap et al. 2012). Various structural modifications around thiazole core identified its role as an important pharmacophore in many clinically used drugs. Among different synthetic derivatives of 1,3-thiazoles, 2-amino-1,3-thiazoles are an attractive moiety in medicinal chemistry with a wide spectrum of biological activities (Das et al. 2016; Cheng et al. 2016; Gallardo-Godoy et al. 2011; Gorczyński et al. 2004). Our research group has been interested in the design, virtual screening, synthesis, and biological evaluation of novel heterocyclic tumor growth inhibitors and apoptosis inducers as potential new anticancer agents. The recurrence of 2-aminothiazole motif in a number of compounds with reported anticancer activities such as DAT1 and related compounds (Sengupta et al. 2005; Romagnoli et al. 2009; Paula et al. 2013) motivated us to select 2-aminothiazole as a template for the design of a novel scaffold for anticancer drug design.

For enriching biologically relevant chemical space (BRCS) around the 2-aminothiazole core, we were encouraged by the growing interest in hydrazones with varied physical, chemical, and biological activities (Rollas and Küçükgül 2007; Tian et al. 2010) along with expanding knowledge in their potential anticancer activities, (Green et al. 2001; Kalinowski et al. 2007; Lovejoy and Richardson 2002; Dandawate et al. 2014; Nasr et al. 2014; Kapláneš et al. 2015a, b; Yu et al. 2015), especially thiazolyl hydrazones (Novinson et al. 1976; Holla et al. 2003; Savini et al. 2004; Altıntop et al. 2014; Dilek Altıntop et al. 2014). Our continued interest in the synthesis and biological evaluations of thiazole compounds, especially 2,4-diamino-5-ketothiazoles, and intensifying our research further, we designed the next higher homolog of DAT1 by providing an azomethine linkage at

C4 which resulted in 2-amino-4-alkylidene/arylidenehydrazino-5-benzoyl-1,3-thiazoles (HAT) and accomplished a one pot synthetic protocol (Titus and Sreejalekshmi 2014) to access these compounds. The broad structural diversity encompassed by these novel entities store immense potential for lead generation in chemical genetics and drug discovery.

The present article describes the synthesis of a series of HAT and their *in vitro* anticancer activity against six NCI approved human cancer cell lines. Expansion of the chemical space around the scaffold was carried out by the design of a 200-member virtual combinatorial HAT library (VCHATL) and *in silico* screening in well-established anticancer target proteins viz; estrogen receptor (3ERT), cyclin dependent kinase (CDK1), and aurora kinase (3LAU). It is worth noting that the predicted ADME properties further highlight the potential of the designed scaffold in anticancer drug design and development.

Materials and methods

Experimental

Aminoguanidine nitrate (AGN) isothiocyanates, α -bromoketones and CDCl_3 were purchased from Aldrich chemical company and were used as such. Ketones/aldehydes,

DMF, DMSO, Et_3N , and NaOH were purchased from Merck chemicals and the solvents were purified using general procedure. Silica-coated plates for thin layer chromatography (TLC) were obtained from Merck, India, and spots were visualized under ultraviolet (UV) light or in iodine chamber. All the synthesized compounds were characterized by spectroscopic techniques (^1H nuclear magnetic resonance (NMR), ^{13}C NMR, mass spectrometry (MS), Fourier transform infrared (FT-IR)), melting point (mp) determination and elemental analysis. Mp determination was carried out using ThermoScientific mp apparatus. NMR spectra were recorded using Bruker AV III 500 MHz FT-NMR spectrometer using CDCl_3 as solvent. Liquid chromatography/mass spectrometry (LC/MS) spectra were recorded on Varian Inc LC/MS spectrometer. HR-MS was obtained using Waters Micromass Q-TofmicroTM (YA105) spectrometer. Electrospray ionization-mass spectrometry (ESI-MS) was recorded using ThermoScientific ExactiveOrbitrap mass spectrometer. Infrared (IR) spectra were obtained using Perkin Elmer Spectrum 100 FT-IR spectrometer. Elemental analysis was carried out with Perkin Elmer 2400 Series CHNS/O Analyzer.

Synthesis

General procedure for the synthesis of 2-amino-4-alkylidene/arylidenehydrazino-5-benzoyl-1,3-thiazoles (HAT)

The HATs were synthesized by [4 + 1] ring closure between a C–N–C–S fragment aminoamidinothiourea (AATU) and α -halo ketone. AATUs were synthesized by treating a suspension of aminoguanidine nitrate (10 mmol, 1.37 g) and NaOH (10 mmol, 0.40 g) in DMF for 10 min at room temperature followed by the addition of 10 mmol of the ketone/aldehyde and further stirring for 45–50 min. Further, isothiocyanate (9 mmol) in DMF was added drop wise and stirred for 1 h followed by addition of the mixture to crushed ice for the precipitation of the solid product. AATU was purified and isolated by recrystallization from appropriate solvents. In the ring closure step, AATU (10 mmol) in DMSO and α -bromoketone (10 mmol) were reacted in presence of 1.2 molar excess of Et₃N for 10 min at room temperature and then was added to crushed ice to obtain the solid HAT which was collected by filtration, air-dried and purified by recrystallization from suitable solvents.

5-Benzoyl-4-isopropylidenehydrazino-2-phenylaminothiazole (1a) Yellow solid (EtOH–CH₃COCH₃, 1:1). (The required AATU was synthesized using acetone (10 mmol, 0.580 g), AGN (10 mmol, 1.37 g) and phenylisothiocyanate (9 mmol, 1.21 g) following the general procedure. The isolated product after recrystallization from EtOH/Water (1:1) was treated with phenacylbromide (10 mmol, 1.99 g) in presence of Et₃N following the general procedure. The crude product was purified by recrystallization using ethanol–acetone (1:1) mixture to obtain the pure product as yellow solid). Yield 97%; mp 206–208 °C; IR (UATR) ν_{\max} : 3350, 3220, 3060, 1676, 749, and 690 cm⁻¹; ¹H NMR (CDCl₃, 500 MHz, ppm): δ = 12.09 (s, 1NH), 8.45 (s, 1ArNH), 7.76–7.77 (m, 1ArH), 7.40–7.48 (m, 5ArH), 7.28–7.29 (m, 3ArH), 7.21–7.24 (m, 1ArH), 2.10 (s, 6H, CH₃); ¹³C NMR (CDCl₃, 67.9 MHz, ppm): δ = 184.2 (C, C-10), 161.8 (C, C-2), 152.3 (C, C-4), 141.3 (C, C-17), 138.2 (C, C-6), 130.7 (C, C-5), 129.7 (C, C-12), 128.4 (C, C-14), 127.2 (C, C-8, C-13), 125.6 (C, C-9), 120.9 (C, C-7), 94.4 (C, C-11), 25.2 (C, C-16), 17.2 (C, C-15); EIMS m/z 350 [M]⁺ (40), 245 (6), 119 (21), 105 (37), 77 (100), 56 (19); anal. calcd. for C₁₉H₁₈N₄O₂S: C, 65.12; H, 5.18; N, 15.99. Found: C, 65.08; H, 5.14; N, 15.83.

5-Benzoyl-4-isopropylidenehydrazino-2-(4-methoxyphenylamino)thiazole (1b) Yellow solid (EtOH–CH₃COCH₃, 1:1). (The desired AATU was synthesized using acetone (10 mmol, 0.580 g), AGN (10 mmol, 1.37 g) and

4-methoxyphenylisothiocyanate (9 mmol, 1.48 g). The isolated product after purification by recrystallization (EtOH/Water-1:1) was then reacted with phenacylbromide (10 mmol, 1.99 g) following the general procedure and pure **1b** was obtained after recrystallization from ethanol–acetone (1:1) mixture as yellow solid). Yield 92%; mp 238–240 °C; IR (UATR) ν_{\max} : 3268, 3076, 2996, 1695, 1231, and 1030 cm⁻¹; ¹H NMR (CDCl₃, 500 MHz, ppm): δ = 12.08 (s, 1NH), 8.95 (s, 1ArNH), 7.74–7.76 (m, 2ArH), 7.41–7.46 (m, 3ArH), 7.25–7.28 (m, 1ArH), 6.86–6.88 (m, 1ArH), 6.82–6.83 (m, 1ArH), 6.72–6.76 (m, 1ArH), 3.79 (s, 3H, OCH₃), 2.03 (s, 3H, CH₃), 1.97 (s, 3H, CH₃); ¹³C NMR (CDCl₃, 125 MHz, ppm): δ = 183.8 (C, C-10), 171.9 (C, C-9), 162.0 (C, C-2), 152.2 (C, C-4), 141.2 (C, C-17), 135.8 (C, C-14), 135.6 (C, C-6), 130.5 (C, C-5), 130.2 (C, C-12), 128.2 (C, C-13), 127.1 (C, C-7), 121.5 (C, C-8), 94.6 (C, C-11), 55.4 (C, C-18), 25.0 (C, C-16), 17.1 (C, C-15); EIMS m/z 364[M]⁺ (100), 308 (20), 259 (23), 133 (48), 132 (34), 105 (63), 91 (16), 77 (37), 56 (48); anal. calcd. for C₂₀H₂₀N₄O₂S: C, 65.90; H, 5.53; N, 15.37. Found: C, 65.77; H, 5.46; N, 15.29.

5-(4-Fluorobenzoyl)-4-isopropylidenehydrazino-2-phenylaminothiazole (1c) Yellow solid (EtOH–CH₃COCH₃, 1:1). (The corresponding AATU was obtained using acetone (10 mmol, 0.580 g), AGN (10 mmol, 1.37 g) and phenylisothiocyanate (9 mmol, 1.21 mg) and following the general procedure. It was purified by recrystallization using EtOH/Water (1:1) and then treated with 4-fluorophenacylbromide (10 mmol, 2.77 g). It was purified by recrystallization using ethanol–acetone (1:1) mixture to obtain pure yellow solid). Yield 90 %; mp 224–225 °C; IR (UATR) ν_{\max} : 3340, 3279, 3062, 2945, 1670, 847, and 755 cm⁻¹; ¹H NMR (CDCl₃, 500 MHz, ppm): δ = 12.08 (s, 1NH), 9.10 (s, 1ArNH), 7.76–7.80 (m, 2ArH), 7.38–7.42 (m, 2ArH), 7.28–7.30 (m, 2ArH), 7.21–7.24 (m, 1ArH), 7.12 (t, J = 8.5 Hz, 2ArH), 2.03 (s, 3H, CH₃), 1.96 (s, 3H, CH₃); ¹³C NMR (CDCl₃, 125 MHz, ppm): δ = 182.6 (C, C-10), 171.4 (C, C-14), 165.0 (C, C-13), 163.0 (C, C-5), 162.1 (C, C-2), 152.4 (C, C-4), 138.4 (C, C-17), 137.4 (C, C-6), 129.5 (C, C-8), 125.8 (C, C-9), 121.4 (C, C-12), 115.5 (C, C-7), 95.0 (C, C-11), 24.9 (C, C-16), 17.1 (C, C-15); anal. calcd. for C₁₉H₁₇FN₄OS: C, 61.94; H, 4.65; N, 15.22. Found: C, 59.37; H, 3.88; N, 14.45.

4-Isopropylidenehydrazino-2-(4-methoxyphenylamino)-5-(naphth-2-oyl)thiazole (1e) Yellow solid (EtOH–CH₃COCH₃, 1:1). (The desired AATU was synthesized using acetone (10 mmol, 0.580 g), AGN (10 mmol, 1.37 g) and 4-methoxyphenylisothiocyanate (9 mmol, 1.48 g) following the general procedure. The purified product obtained by recrystallization (EtOH/Water-1:1) was then treated with 2-bromoacetyl naphthalene (10 mmol, 2.49 g) following the

general procedure. The crude product was purified by recrystallization using ethanol–acetone (1:1) mixture to obtain the product as yellow solid). Yield 90 %; mp 223–224 °C. IR (UATR) ν_{\max} : 3395, 3269, 3054, 2996, 1636, 1231, 1030, 823, and 776 cm^{-1} ; ^1H NMR (CDCl_3 , 500 MHz, ppm): δ = 12.19 (s, 1NH), 8.29 (s, 1ArNH), 8.20 (s, 1ArH), 7.87–7.91 (m, 1ArH), 7.84–7.86 (m, 2ArH), 7.80–7.82 (m, 1ArH), 7.49–7.55 (m, 2ArH), 7.21–7.22 (m, 2ArH), 6.89–6.90 (m, 2ArH), 3.80 (s, 3H, OCH_3), 2.08 (s, 6H, CH_3); ^{13}C NMR (CDCl_3 , 125 MHz, ppm): δ = 183.8 (C, C-10), 173.4 (C, C-9), 162.5 (C, C-2), 158.2 (C, C-23), 152.3 (C, C-4), 138.8 (C, C-6), 134.3 (C, C-5), 132.6 (C, C-12), 131.2 (C, C-13, C-18), 128.9 (C, C-14), 128.3 (C, C-15), 127.7 (C, C-16), 127.3 (C, C-17), 126.5 (C, C-19), 124.7 (C, C-7, C-20), 114.9 (C, C-8), 95.0 (C, C-11), 55.5 (C, C-24), 25.2 (C, C-21), 17.3 (C, C-22); LCMS m/z : 430.15 $[\text{M}]^+$.

4-isopropylidenehydrazino-5-(naphth-2-oyl)-2-phenylaminothiazole (**1f**) Yellow solid ($\text{EtOH}-\text{CH}_3\text{COCH}_3$, 1:1). (The corresponding AATU was obtained by the reaction between acetone (10 mmol, 0.580 g), AGN (10 mmol, 1.37 g) and phenylisothiocyanate (9 mmol, 1.21 g). The recrystallized product (EtOH/Water -1:1) was then treated with 2-bromoacetylnaphthalene (10 mmol, 2.49 g) following the general procedure. The crude product was purified by recrystallization using ethanol–acetone (1:1) mixture to obtain the product as yellow solid). Yield 90%; mp 258–259 °C; IR (UATR) ν_{\max} : 3282, 3098, 3052, 1629, 832, and 759 cm^{-1} ; ^1H NMR (CDCl_3 , 500 MHz, ppm): δ = 12.15 (s, 1NH), 8.24 (s, 1ArH), 8.19 (s, 1ArNH), 7.90–7.93 (m, 2ArH), 7.83–7.88 (m, 2ArH), 7.51–7.57 (m, 2ArH), 7.37–7.41 (m, 2ArH), 7.25–7.27 (m, 2ArH), 7.19–7.22 (m, 1ArH), 2.16 (s, 3H, CH_3), 2.12 (s, 3H, CH_3); ^{13}C NMR (CDCl_3 , 125 MHz, ppm): δ = 184.1 (C, C-10), 171.2 (C, C-9), 161.9 (C, C-2), 152.4 (C, C-4), 138.7 (C, C-23), 138.2 (C, C-12), 134.4 (C, C-5), 132.6 (C, C-6), 129.7 (C, C-18), 128.9 (C, C-14), 128.4 (C, C-20), 127.8 (C, C-15), 127.4 (C, C-16), 126.6 (C, C-17), 125.6 (C, C-19), 124.3 (C, C-8), 120.9 (C, C-7), 95.0 (C, C-11), 25.2 (C, C-21), 17.3 (C, C-22); LCMS m/z : 400.12 $[\text{M}]^+$.

5-Benzoyl-4-isobutylidenehydrazino-2-(4-methoxyphenylamino)thiazole (**2b**) Yellow solid ($\text{EtOH}-\text{CH}_3\text{COCH}_3$, 1:1). (The AATU for the synthesis of **2b** was obtained by reacting 2-butanone (10 mmol, 0.721 g), AGN (10 mmol, 1.37 g) and 4-methoxyphenylisothiocyanate (9 mmol, 1.48 g) following the general reaction procedure. The purified AATU (recrystallization using EtOH/Water -1:1) was then treated with phenacylbromide (10 mmol, 1.99 g) and the crude product obtained on work up was purified by recrystallization using ethanol–acetone (1:1) mixture to obtain the product as yellow solid). Yield 80%; mp

217–218 °C; IR (UATR) ν_{\max} : 3268, 3201, 2870, 1698, 836, and 729 cm^{-1} ; ^1H NMR (CDCl_3 , 500 MHz, ppm): δ = 12.12 (s, 1NH), 8.32 (s, 1ArNH), 7.71 (d, J = 7.0 Hz, 2ArH), 7.36–7.45 (m, 3ArH), 7.20–7.22 (m, 2ArH), 6.89–6.93 (m, 2ArH), 3.81 (s, 3H), 2.44–2.46 (m, 1H), 2.33–2.36 (m, 1H), 2.06 (s, 3H), 2.01–2.05 (m, 1H), 1.09–1.23 (m, 2H); ^{13}C NMR (CDCl_3 , 125 MHz, ppm): δ = 183.7 (C, C-10), 173.0 (C, C-9), 162.5 (C, C-2), 156.7 (C, C-18), 152.1 (C, C-4), 141.4 (C, C-6), 131.1 (C, C-5), 130.5 (C, C-13), 128.4 (C, C-12), 127.2 (C, C-14), 124.7 (C, C-7), 114.7 (C, C-8), 94.6 (C, C-11), 55.5 (C, C-19), 31.9 (C, C-15), 24.1 (C, C-17), 17.2 (C, C-16); LCMS m/z : 393.30 $[\text{M} - 1]^+$.

4-Isobutylidenehydrazino-5-(naphth-2-oyl)-2-phenylaminothiazole (**2d**) Yellow solid ($\text{EtOH}-\text{CH}_3\text{COCH}_3$, 1:1). (The AATU for **2d** was synthesized using 2-butanone (10 mmol, 0.721 g), AGN (10 mmol, 1.37 g) and phenylisothiocyanate (9 mmol, 1.21 g). The product was recrystallized using EtOH/Water (1:1) and then treated with 2-bromoacetylnaphthalene (10 mmol, 2.49 g) following the general procedure. The crude product was purified by recrystallization using ethanol–acetone (1:1) mixture to obtain the product as yellow solid). Yield 90%; mp 237–238 °C; IR (UATR) ν_{\max} : 3282, 3098, 3052, 1629, 832, and 759 cm^{-1} ; ^1H NMR (CDCl_3 , 500 MHz, ppm): δ = 12.13 (s, 1NH), 8.24 (s, 1ArH), 8.53 (s, 1ArNH), 7.89–7.92 (m, 3ArH), 7.83–7.88 (m, 3ArH), 7.51–7.57 (m, 3ArH), 7.36–7.39 (m, 2ArH), 2.39 (dd, J = 7.5 Hz, 2H), 2.08 (s, 3H), 1.13 (t, J = 7.5 Hz, 3H); ^{13}C NMR (CDCl_3 , 125 MHz, ppm): δ = 184.1 (C, C-10), 171.2 (C, C-9), 161.9 (C, C-2), 156.8 (C, C-4), 138.7 (C, C-23), 138.3 (C, C-12), 134.4 (C, C-5), 132.6 (C, C-6), 129.7 (C, C-18), 128.9 (C, C-14), 128.4 (C, C-20), 127.8 (C, C-15), 127.4 (C, C-16), 126.6 (C, C-17), 125.6 (C, C-19), 124.3 (C, C-8), 120.9 (C, C-7), 95.1 (C, C-11), 32.1 (C, C-15), 15.2 (C, C-17), 11.4 (C, C-16); LCMS m/z : 414.10 $[\text{M}]^+$.

5-Benzoyl-4-cyclohexylidenehydrazino-2-(4-methoxyphenylamino)thiazole (**3b**) Yellow solid ($\text{EtOH}-\text{CH}_3\text{COCH}_3$, 1:1). (The desired AATU was synthesized using cyclohexanone (10 mmol, 0.981 g), AGN (10 mmol, 1.37 g) and 4-methoxyphenylisothiocyanate (9 mmol, 1.48 g) following the general procedure. The product after recrystallization (EtOH/Water -1:1) was reacted with phenacylbromide (10 mmol, 1.99 g) following the general procedure. The crude product was purified by recrystallization using ethanol–acetone (1:1) mixture to obtain the product as yellow solid). Yield 80%; mp. 246–247 °C; IR (UATR) ν_{\max} : 3276, 3198, 2938, 2858, 1678, 831, and 731 cm^{-1} ; ^1H NMR (CDCl_3 , 500 MHz, ppm): δ = 12.34 (s, 1NH), 8.36 (s, 1ArNH), 7.70–7.72 (m, 2ArH), 7.38–7.47 (m, 3ArH), 7.20–7.22 (m, 2ArH), 6.89–6.92 (m, 2ArH), 3.81 (s, 3H),

2.49–2.52 (m, 2H), 2.34–2.38 (m, 2H), 1.63–1.72 (m, 6H); ^{13}C NMR (CDCl_3 , 125 MHz, ppm): δ = 183.7 (C, C-10), 173.4 (C, C-9), 162.8 (C, C-2), 158.3 (C, C-15), 158.2 (C, C-4) 141.4 (C, C-6), 131.2 (C, C-13), 130.5 (C, C-5), 128.4 (C, C-12), 127.2 (C, C-14), 124.7 (C, C-7), 114.9 (C, C-8), 94.6 (C, C-11), 55.5 (C, C-19), 35.2 (C, C-16), 27.2 (C, C-16'), 26.9 (C, C-17), 25.6 (C, C-17'), 25.9 (C, C-18); LCMS m/z : 421.12 $[\text{M} + 1]^+$.

4-Cyclohexylidenehydrazino-5-(4-methoxybenzoyl)-2-phenylaminothiazole (**3c**) Yellow solid (EtOH– CH_3COCH_3 , 1:1). (The corresponding AATU was synthesized using cyclohexanone (10 mmol, 0.981 g), AGN (10 mmol, 1.37 g) and phenylisothiocyanate (9 mmol, 1.21 g). The recrystallized product (EtOH/Water-1:1) and 4-methoxyphenacylbromide (10 mmol, 2.29 g) was reacted following the general procedure. The crude product was purified by recrystallization using ethanol–acetone (1:1) mixture to obtain the product as yellow solid). Yield 63%; mp 224–225 °C; IR (UATR) ν_{max} : 3296, 1629, 1545, 1244, and 1058 cm^{-1} ; ^1H NMR (CDCl_3 , 500 MHz, ppm): δ = 12.29 (s, 1NH), 8.38 (s, 1ArNH), 7.75–7.77 (m, 2ArH), 7.38–7.42 (m, 2ArH), 7.27–7.28 (m, 2ArH), 7.19–7.22 (m, 1ArH), 6.92–6.94 (m, 2ArH), 3.85 (s, 3H), 2.51–2.53 (m, 2H), 2.40–2.43 (m, 2H), 0.69–1.75 (m, 4H); ^{13}C NMR (CDCl_3 , 125 MHz, ppm): δ = 183.4 (C, C-10), 170.9 (C, C-14), 161.9 (C, C-2), 161.6 (C, C-14), 156.2 (C, C-15), 151.9 (C, C-4), 138.5 (C, C-17), 133.8 (C, C-5), 133.7 (C, C-13), 129.6 (C, C-8), 129.2 (C, C-6), 125.5 (C, C-9), 121.1 (C, C-12), 113.7 (C, C-7), 98.0 (C, C-11), 55.4 (C, C-19), 31.9 (C, C-16), 24.1 (C, C-16'), 17.2 (C, C-17), 15.2 (C, C-17'), 11.3 (C, C-18); ESIMS m/z : 421.16 $[\text{M} + \text{H}]^+$; anal. calcd. for $\text{C}_{23}\text{H}_{24}\text{N}_4\text{O}_2\text{S}$: C, 65.69; H, 5.76; N, 13.33. Found: C, 66.18; H, 5.91; N, 13.55.

5-Benzoyl-4-benzylidenehydrazino-2-(4-methoxyphenylamino)thiazole (**4b**) Yellow solid (EtOH– CH_3COCH_3 , 1:1). (The required AATU was synthesized using benzaldehyde (10 mmol, 1.06 g), AGN (10 mmol, 1.37 g) and 4-methoxyphenyl isothiocyanate (9 mmol, 1.48 g) following the general procedure. Then the recrystallized product (EtOH/Water-1:1) was treated with phenacylbromide (10 mmol, 1.99 g) following the general procedure. The crude product was purified by recrystallization using ethanol–acetone (1:1) mixture to obtain **4b** as yellow solid). Yield 85%; mp 193–194 °C; IR (UATR) ν_{max} : 3220, 3040, 1718, 826, and 725 cm^{-1} ; ^1H NMR (CDCl_3 , 500 MHz, ppm): δ = 12.39 (s, 1NH), 8.05 (s, 1ArNH), 7.98 (s, 1H), 7.64–7.67 (m, 3ArH), 7.51–7.54 (m, 3ArH), 7.46–7.48 (m, 2ArH), 7.35–7.42 (m, 3ArH), 7.23–7.31 (m, 1ArH), 6.94 (d, J = 9 Hz, 2ArH), 3.83 (s, 3H); ^{13}C NMR (CDCl_3 , 125 MHz, ppm): δ = 184.2 (C, C-10), 173.6 (C, C-9), 161.8 (C, C-2), 158.0 (C, C-19), 155.4 (C, C-4), 141.3 (C, C-6), 133.8 (C, C-15), 131.3 (C, C-5), 130.7 (C, C-8), 129.6 (C, C-12),

128.4 (C, C-13), 128.2 (C, C-14), 128.3 (C, C-16), 127.3 (C, C-16), 127.2 (C, C-7), 124.8 (C, C-17), 114.4 (C, C-18), 94.6 (C, C-11), 55.4 (C, C-20); LCMS m/z : 429.30 $[\text{M} + 1]^+$.

In vitro anticancer screening

The compounds were screened for their anticancer activity using the colorimetric sulforhodamine B (SRB) assay following the reported protocol (Skehan et al. 1990; Vichai and Kirtikara 2006). Six human cancer cell lines namely MCF-7, SW-620, HL-60, A549, OVCAR-3, and SK-MEL-2 were selected from the NCI's (National Cancer Institute) cell line panel. Three consecutive screening experiments were carried out for each compound in a 96-well plate (5×10^3 cells/well). The dose-response in each of the experiments was measured at four different concentrations (10, 20, 40, and 80 $\mu\text{g}/\text{mL}$) of the compounds in DMSO or alcohol and in each experiment Adriamycin (ADR) was used as a positive control at the same concentration levels. The percentage growth was evaluated spectrophotometrically against controls that were not treated with test compounds.

Virtual screening

All the computational studies were carried out using Schrodinger software suite 2014 (Schrodinger LLC 2014). The ligand structures used in this study were constructed using the graphical tool, Maestro 9.6 and geometry optimization and partial atomic charge assignment of ligands were done with the help of Ligprep using the optimized potentials for liquid simulations-all atom (OPLS-AA) force field (Jorgensen et al. 1996). The X-ray crystal structures of proteins were retrieved from RCSB Protein Data Bank (PDB ID codes 3ERT, 3LAU, and 3FDN). Prior to calculations, the raw crystal structures were prepared and the water molecules were removed using protein preparation tool (PrepWizard) in the software package. All docking calculations were performed using the Extra Precision (XP) mode of a grid-based ligand docking method, GLIDE 6.1 (Friesner et al. 2006). The grid was generated in such a way that grid center was located at the mid-point of the longest atom–atom distance in the respective co-crystallized ligand in the protein. The native ligand was used as the reference for the grid generation. Inside the grid, at most 800 poses per ligands were generated keeping the default variables as such. The free energy of binding for each ligand was calculated by the sum of all the interactions like hydrogen bonding, hydrophobic, lipophilic etc. The lowest estimated free energy from various binding conformations of each ligand was calculated, ranked by dock score functions and

the best docked structure was chosen. All the pharmaceutically relevant properties and physical descriptors of the optimized ligands were calculated using Qikprop 3.5 in Schrodinger LLC. The recommended ranges for the descriptors were derived by comparing those with 95% known drugs. The physical descriptor values such as MW, octanol/water partition coefficient, H-bond donor/acceptor were compared with classical Lipinski's RO5 and oral bioavailability was calculated using Caco-2 and MDCK cell membrane models.

Results and discussion

Chemistry

Driven by the success stories on the anticancer activity of 2-aminothiazole derivatives, we felt it worth examining the possibilities of developing unexplored members from this family. Importance of biologically relevant hydrazone libraries, especially hydrazone–heterocycle combinations in drug discovery (Verma et al. 2014) and reported bioactivities of different hydrazone containing thiazoles, exclusively 2-hydrazinothiazoles (Bharti et al. 2010; Secci et al. 2012; Carradori et al. 2013; Yurttas et al. 2013) inspired us to select the hydrazone fragment for the modification of 2-aminothiazole core. In the light of the literature survey, a novel heterocyclic scaffold based on 2-aminothiazole

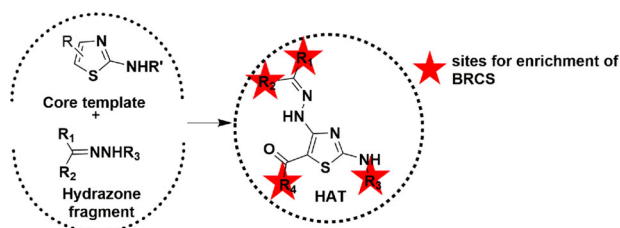
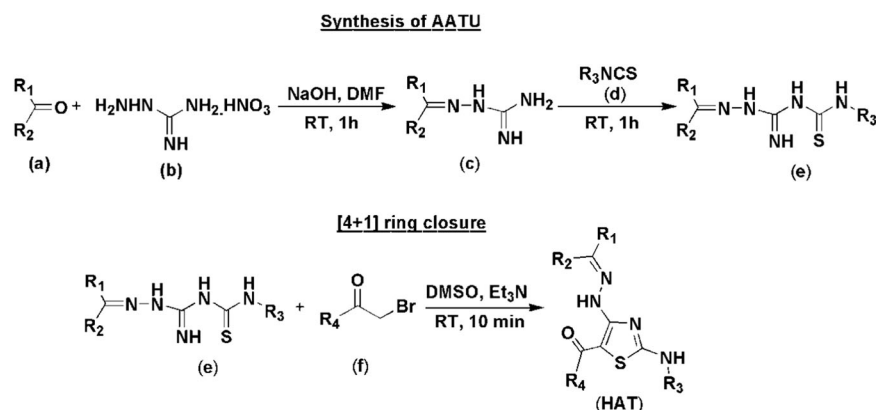


Fig. 1 Novel drug design scaffold combining aminothiazole and hydrazone fragment

Scheme 1 Chemical synthesis of HAT



template was designed by the modification of C4 of the ring with hydrazone fragment to afford HAT. The designed tetravariant scaffold provides four sites for chemical space enrichment around the core. (Fig. 1).

As the synthetic feasibility is a crucial factor in drug discovery, an easy and economically viable synthetic route to the novel scaffold, HAT was accomplished following a [4 + 1] thiazole ring formation (Scheme 1) under mild conditions employing commercially available building blocks to facilitate automated synthetic protocols.

Different sites for diversity multiplication (R_1 , R_2 , R_3 , and R_4) would facilitate vast expansion of HAT library and modification of chemical space around the core. Giving special emphasis on the hydrazone part, by varying R_1 and R_2 , a contribution from carbonyl component, we designed isopropylidene (IPHAT), isobutylidene (IBHAT), cyclohexylidene (CyHAT), and benzylidene (BzHAT) (Fig. 2) derivatives of HAT.

The generality of the synthetic route was established by synthesis of compounds (1–4) in moderate to excellent yields (Table 1), where diversity elements R_1 and R_2 were introduced as capping units in aminoguanidine nitrate (b) by treating with carbonyl compounds (a) and the resultant Schiff bases (c) were condensed with arylisothiocyanate (d) under basic conditions to afford aminoamidinothioureas (e) (Sreejalekshmi 2010) as the C–N–C–S precursors for thiazole ring synthesis. In the second step, these C–N–C–S precursors underwent a base assisted elimination–cyclization–aromatization with α -bromoketones (f) at room temperature to afford the desired compounds in excellent yield. Having representative HAT molecules in our hands, we next proceeded with the investigation of their potential as anticancer agents.

In vitro anticancer screening

The cytotoxicity of 12 compounds were evaluated in cancer cell lines—MCF-7, HL-60, SK-MEL-2, A549, OVCAR-3, and SW620 using SRB assay with Adriamycin (ADR) as

Fig. 2 Four classes of HAT scaffold by varying carbonyl component

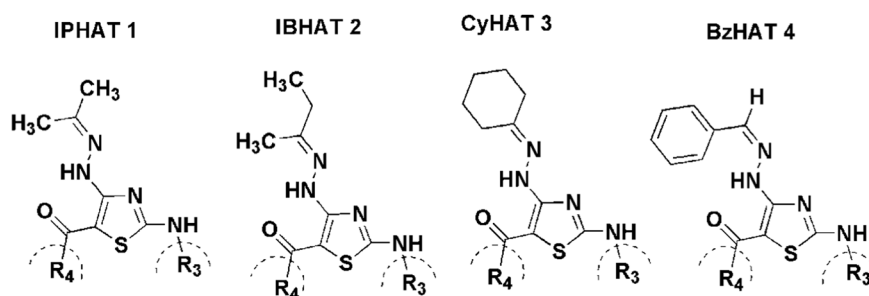


Table 1 Synthesized HAT molecules

Compound	R ₁	R ₂	R ₃	R ₄	% Yield
1a	–CH ₃	–CH ₃	–C ₆ H ₅	–C ₆ H ₅	97
1b	–CH ₃	–CH ₃	4-OMeC ₆ H ₄	–C ₆ H ₅	92
1c	–CH ₃	–CH ₃	–C ₆ H ₅	4-FC ₆ H ₄	90
1d^a	–CH ₃	–CH ₃	–C ₆ H ₅	4-ClC ₆ H ₄	94
1e	–CH ₃	–CH ₃	4-OMeC ₆ H ₄	–C ₁₂ H ₁₁	90
1f	–CH ₃	–CH ₃	–C ₆ H ₅	–C ₁₂ H ₁₁	90
2b	–CH ₃	–C ₂ H ₅	4-OMeC ₆ H ₄	–C ₆ H ₅	80
2c^a	–CH ₃	–C ₂ H ₅	–C ₆ H ₅	4-OMeC ₆ H ₄	88
2d	–CH ₃	–C ₂ H ₅	–C ₆ H ₅	–C ₁₂ H ₁₁	90
3b	–C ₆ H ₁₀		4-OMeC ₆ H ₄	–C ₆ H ₅	80
3c	–C ₆ H ₁₀		–C ₆ H ₅	4-OMeC ₆ H ₄	63
4b	–C ₆ H ₅	H	4-OMeC ₆ H ₄	–C ₆ H ₅	85

^a Reported earlier (Titus and Sreejalekshmi 2014)

the positive control and reference. The screening results suggested the breast cancer cell line, MCF-7, to be more fragile towards our tested compounds where GI₅₀ values were <40 µg/mL. Comparison of cytotoxicity of the tested compounds is presented in Table 2. Among the tested compounds, the IBHAT derivative-5-benzoyl-4-isobutylidenehydrazino-2-(4-methoxyphenylamino)thiazole (**2b**) and the BzHAT derivative-5-benzoyl-4-benzylidenehydrazino-2-(4-methoxyphenylamino)thiazole (**4b**) displayed anticancer activity against MCF-7 (Fig. 3a) with GI₅₀ values of 2.32 and 8.16 µg/mL respectively, whereas, the CyHAT counterpart-5-benzoyl-4-cyclohexylidenehydrazino-2-(4-methoxyphenylamino)thiazole (**3b**) was active against lung cancer cell line A549 (Fig. 3b) with GI₅₀ value of 1.61 µg/mL. Moreover, all the three active molecules were found to have potent anticancer activity against all the tested cell lines. IPHAT derivative-5-benzoyl-4-isopropylidenehydrazino-2-(4-methoxyphenylamino)thiazole (**1b**) showed moderate anticancer activity against MCF-7 and HL60 cell lines with GI₅₀ = 35.60 and 33.64 µg/mL respectively and was inactive against the other cell lines tested.

It was interesting to note that most of tested compounds showed selective dose-response towards the breast, leukemia and/or lung cancer cell lines whereas the colon,

ovarian, and skin melanoma cancer cells were found to be less affected. Considering these facts, we decided to expand the library of HAT and to proceed with the in silico binding studies in anticancer target proteins.

In silico studies

ADME property prediction

The bioavailability of the test molecules was assessed by ADME (absorption, distribution, metabolism, and excretion) prediction using Qikprop which relies mainly on Lipinski Rule-of-Five and Jorgensen rule-of-three violations. The pharmaceutically relevant properties—octanol/water and water/gas log Ps, log S, log BB, overall CNS activity, Caco-2 and MDCK cell permeabilities, and human oral absorption were calculated (Table 3) and compared with those of existing drugs. All the compounds showed properties within the recommended range for 95% of drugs which suggested the drug-likeness of the designed molecules with theoretically good passive oral absorption.

Molecular docking

With the aim of enriching BRCS, an in-house 200-member virtual combinatorial HAT library (VCHATL) was designed by varying R₃ and R₄ in the respective parent structures (**1a–4a**) of IPHAT, IBHAT, CyHAT, and BzHAT which can be realized through the appropriate reagents during the synthesis (Table 4).

To further establish the appropriateness of HAT library in anticancer drug development, molecular docking studies were performed in three different classes of anticancer target proteins. Suitable X-ray crystal structures of the selected proteins—estrogen receptor (PDB ID: 3ERT), Cyclin dependent kinase (PDB ID: 3FDN) and Aurora kinase (PDB ID: 3LAU) were obtained from the protein data bank (PDB) and optimized to get the lowest energy 3D structures. VCHATL was also optimized and screened in the active sites of individual proteins in a grid-based ligand docking protocol using GLIDE and results are presented in Table 5. The docking studies revealed better affinity of CyHAT, in

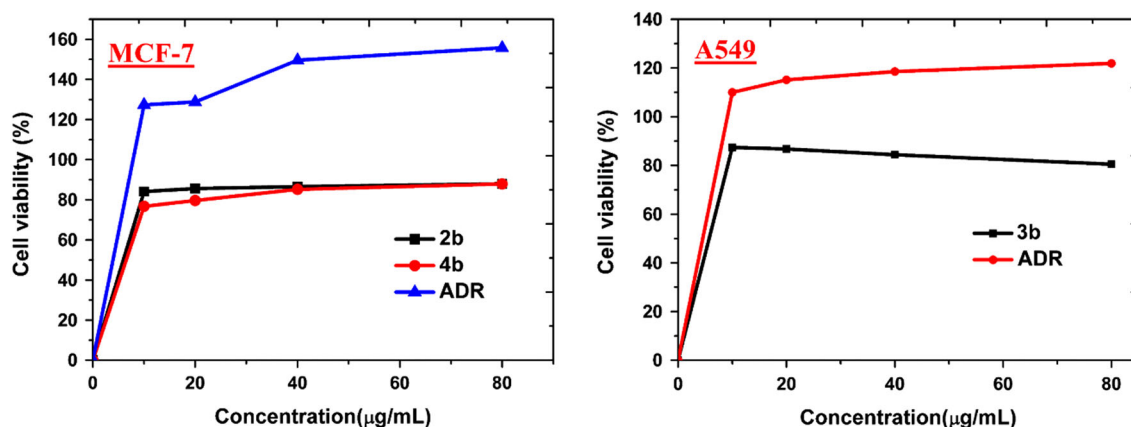
Table 2 In vitro screening results of tested compounds

Compound	GI ₅₀ (μg/mL) ^a					
	MCF-7	SW620	A549	HL60	SK-MEL-2	OVCAR-3
1a	>80	>80	>80	>80	>80	>80
1b	35.6 ± 2.73	78.2 ± 15.05	51.7 ± 4.26	33.6 ± 21.39	>80	>80
1c	>80	>80	>80	>80	>80	>80
1d	>80	>80	>80	>80	>80	>80
1e	34.6 ± 4.04	>80	>80	>80	>80	>80
1f	40.6 ± 5.51	>80	>80	>80	>80	>80
2b	2.32 ± 3.15^c	40.1 ± 5.85	12.5 ± 1.33	30.2 ± 17.14	36.1 ± 1.69	55.0 ± 38.96
2c	>80	>80	43.8 ± 12.72	>80	>80	27.9 ± 2.67
2d	58.8 ± 4.03	>80	>80	41.2 ± 9.73	>80	>80
3b	17.3 ± 3.46	30.7 ± 4.81	1.61 ± 1.41^c	36.4 ± 7.04	16.1 ± 1.95	22.70 ± 4.72
3c	>80	>80	>80	>80	>80	>80
4b	8.16 ± 2.69^c	44.1 ± 6.23	28.7 ± 2.00	38.3 ± 10.61	31.9 ± 0.31	36.1 ± 2.25
ADR ^b	<10	<10	<10	31.3 ± 11.78	<10	<10

^a The values are the mean ± standard deviation (SD) of three independent experiments performed

^b Positive control

^c Marked in bold indicated a pronounced anticancer activity

**Fig. 3** Cell viability of active compounds at different concentrations against **a** MCF-7, **b** A549

terms of binding scores, towards estrogen receptor protein whereas BzHAT class had more affinity to Cyclin dependent kinase protein. But, considering the whole VCHATL, all the members indicated comparatively good affinity towards the active site of Aurora kinase (AURK) protein 3LAU.

Encouraged by higher binding energy of VCHATL in 3LAU protein, we carried out detailed binding studies of the library in AURK proteins. Understanding the role of Aurora kinases in cell cycle and tumorigenesis (Urich et al. 2013) and the inhibition of Aurora kinase activity by small molecule ATP competitors is a widely explored and challenging regime in target-based anticancer therapy (Fancelli et al. 2006; Carpinelli et al. 2007; Manfredi et al. 2007; Mortlock et al. 2007; Wilkinson et al. 2007). In order to

have selective and potent inhibitors, it is essential to understand the molecular constraints of ATP binding hinge region of AURK and the structural basis for its interactions with inhibitors in detail.

Effect of hydrazone substitution on binding affinity

The effect of the hydrazone part in the in silico binding of compounds was evaluated by the detailed binding study of core compounds **1a**, **2a**, **3a**, and **4a** each representing a particular class of HAT –IPHAT, IBHAT, CyHAT, and BzHAT respectively. The predicted binding modes in the active site of the protein (Fig. 4) were interesting where a difference in the binding pattern was observed with respect to variations in R₁ and R₂.

Table 3 Comparison of ADME properties of anticancer active HAT

Ligand	MW	Donor HB	Accept HB	QP Polrz	QP logP o/w	QP log HERG	QPP Caco	QP logBB	#metab	RO5 violations	% Human oral absorption
2b	394.49	1	5.75	41.20	9.241	-6.150	1731	-0.734	3	0	100
3b	420.52	1	5.75	42.85	4.756	-5.794	1428	-0.728	4	0	100
4b	428.50	1	6.25	44.61	4.896	-6.748	1615	-0.742	2	0	100

The molecular weight of the tested ligand, MW (130–725 for 95% drugs); estimated number of H-bonds donated by ligand to water molecules, DonorHB (0–6.0 for 95% drugs); estimated number of H-bonds accepted by ligand from water molecules, AcceptHB (2–20 for 95% drugs); the predicted polarizability, QP polrz (13.0–70.0 for 95 % of drugs); the predicted octanol/water partition coefficient, QP logP o/w (-2.0 to 6.5); the predicted IC₅₀ value for blockage of HERG K⁺ channels, QP log HERG (concern <-5); the predicted apparent Caco-2 cell permeability, QPP Caco in nm/s (<25 poor, >500 great); the predicted brain/blood partition coefficient, QP log BB (-3.0 to 1.0 for 95% drugs); the number of likely metabolic reactions, #metab (1–8 for 95 % of drugs)

Table 4 Designed VCHATL

R₁	H	-CH ₃										
R₂	-CH ₃	-C ₂ H ₅	-C ₆ H ₅	-C ₆ H ₁₀								
R₃	H	4-ClC ₆ H ₅	4-FC ₆ H ₅	4-OMeC ₆ H ₅	4-NO ₂ C ₆ H ₅	4-MeC ₆ H ₅						
R₄	H	4-ClC ₆ H ₅	4-FC ₆ H ₅	4-OMeC ₆ H ₅	4-NO ₂ C ₆ H ₅	Naphthalene	Coumarin	Indol				

Table 5 Molecular docking results for synthesized library of HAT along with ADR

Compound	3ERT				3FDN				3LAU			
	G-score (kcal/mol)	Lipophilic EvdW	H bond	Electro	G-score (kcal/mol)	Lipophilic EvdW	H bond	Electro	G-score (kcal/mol)	Lipophilic EvdW	H bond	Electro
1a	-4.69	-5.14	0	-0.08	-4.46	-3.78	-0.05	-0.1	-5.52	-3.36	-0.92	-0.21
1b	-4.26	-4.77	-0.22	-0.13	-4.02	-3.54	-0.7	-0.3	-6.93	-3.98	-0.73	-0.23
1c	-5.23	-4.19	-0.97	-0.33	-4.44	-3.32	-1.16	-0.36	-5.34	-3.73	-0.77	-0.2
1d	-2.14	-4.26	-0.03	-0.21	-4.51	-3.81	0	-0.1	-5.37	-4.01	0	-0.09
1e	-6.65	-5.89	-0.22	-0.2	-3.31	-4.54	-1.09	-0.31	-6.61	-4.32	-0.97	-0.27
1f	-6.28	-5.16	-0.7	-0.24	-5.46	-4.43	-0.51	-0.29	-7.77	-4.23	-0.93	-0.43
2b	-2.61	-5.56	0	-0.11	-1.73	-4.01	-0.34	-0.05	-7.58	-4.64	-0.7	-0.17
2c	-6.47	-4.93	-0.74	-0.49	-5.29	-4.39	-0.73	-0.2	-6.29	-3.35	-1.81	-0.57
2d	-6.17	-5.28	0	-0.02	-5.49	-4.09	-1	-0.44	-6.62	-4.23	-0.97	-0.55
3b	-1.69	-4.75	0	-0.07	-0.78	-3.56	-0.56	-0.08	-7.03	-4.35	-0.7	-0.23
3c	-5.69	-4.26	-1.03	-0.3	-6.08	-4.05	-0.49	0.02	-5.87	-4.01	-0.7	-0.18
4b	-4.95	-4.55	-0.57	-0.25	-0.53	-4.13	-0.38	-0.25	-7.76	-4.33	-1.03	-0.3
ADR	-4.78	-1.18	-3.3	-1.33	-4.76	-3.31	-3.48	-0.95	-9.91	-4.34	-3.94	-1.06

Compound **1a** (G -score = -5.52 kcal/mol) with 25 heavy atoms was found to bind to ATP hinge region of the protein using its NH-C-N-C-NH unit for H-bonding between Ala213 and Pro214 which are significant residues (Yan et al. 2011) in AURK inhibition. The azomethine part of the hydrazone as well as the phenyl ring (R_4) were occupied in the solvent exposure regions of the protein active site whereas the phenyl ring (R_3) was completely embedded in the hydrophobic domain. When the chain length in the azomethine part was increased by introducing isobutyl (**2a**, G -score = -6.56 kcal/mol) or cyclohexyl (**3a**, G -score = -6.05 kcal/mol) units, the hydrazono part moved more towards the activation loop having the Ala-Asp-Phe triad

commonly referred to as the DFG motif. The ligands occupied the active site such that R_3 phenyl ring was enclosed in a hydrophobic pocket and the C4 and C2 substituents on thiazole moved out of this pocket and exhibited higher ligand efficiency and binding energy than that of **1a**. In the BzHAT derivative **4a**, H-bonding interaction with Ala 213 was absent and the ligand oriented itself near to the activation loop with hydrazono moiety as well as R_4 proximal to the DFG motif. The lowest binding energy (G -score = 5.09 kcal/mol) of **4a** was attributed to the restricted conformational rotation of the azomethine part. The binding affinity of the molecules in 3LAU followed the order **2a** > **3a** > **1a** > **4a** clearly indicating the role of hydrazono

Fig. 4 3D binding mode of **1a**–**4a** in the active site of 3LAU protein

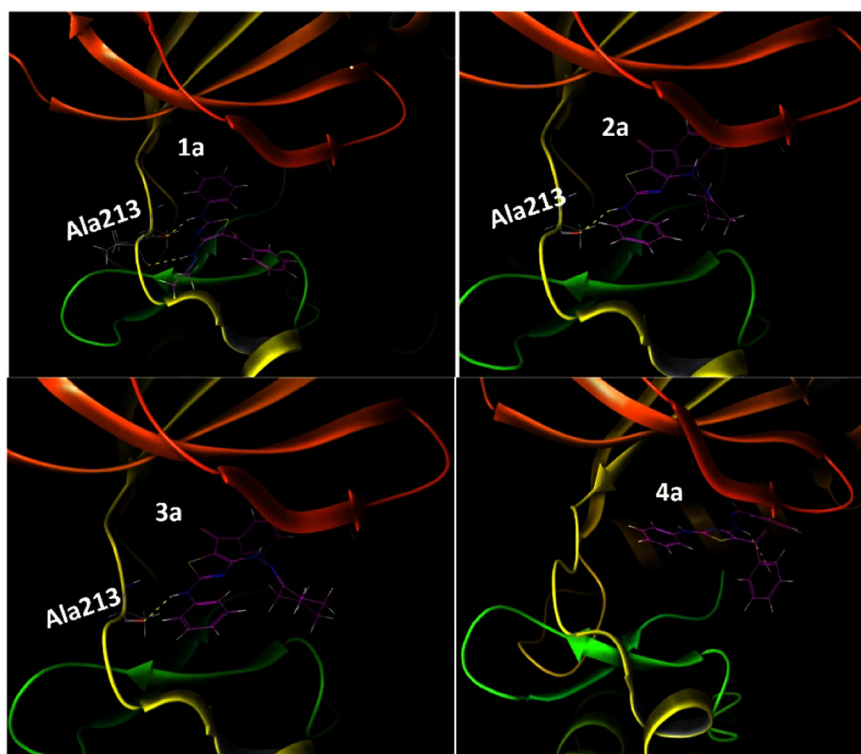
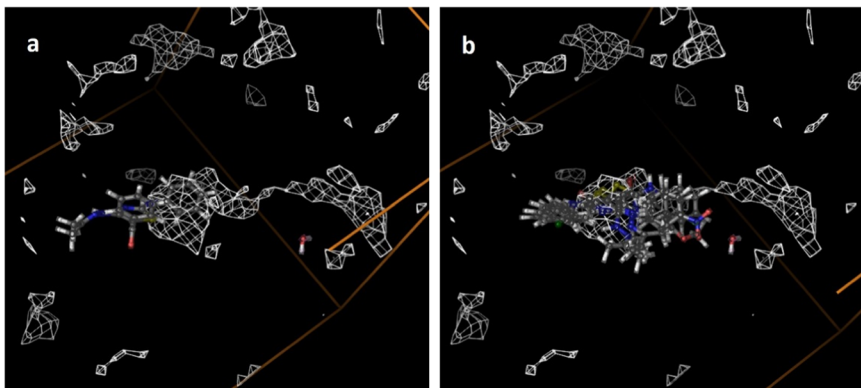


Fig. 5 **a** Hydrophobic enclosure of **1a** in the active site of 3LAU **b** Hydrophobic enclosure of molecules with substituted C2 phenyl groups



moiety in protein binding. It is assumed that the synergic nitrogen atoms in the NH–C–N–C–NH pattern of HAT is stereochemically well suited to form H-bonding interactions with kinase hinge region of the ATP pocket. Since core scaffold from all the four families showed selective binding towards the active site of AURK protein and the scaffold is endowed with additional positions for increasing diversity, the influence of R₃ and R₄ on the binding affinity of molecules inside the active site of 3LAU was next studied.

Effect of R₃ substitution

The hydrophobically enclosed H-bonding with Ala213 imparted more stability to the binding pose of **1a** whereas the expose penalty of the methyl and phenyl group at the

C5 towards the solvent exposure region contributed to its destabilization. But, phenyl ring at C2 was buried inside the hydrophobic enclosure which favored binding of the molecule. When C2 phenyl ring in **1a** was para substituted with different functional groups, rotation of molecule along the C2–NH bond occurred that stabilized orientations of the molecules within hydrophobic enclosure of R₃ with lesser exposure penalty of R₄ (Fig. 5). In all the cases, exposure penalty of the hydrophobic groups were reduced significantly and H-bonding with Ala213 was in the vicinity of the hydrophobic residues of the active site and thus the molecules showed higher binding energies than **1a**.

A similar trend was observed in the case of IBHAT where destabilization caused by solvent exposure of hydrophobic methyl groups was compensated by the interaction between

the C5 phenyl ring and hydrophobic residues of the protein. The molecules were further stabilized by π -cation interaction between Arg137 and C2 phenyl ring with a higher binding energy for molecules with substituted phenyl rings as R₃ (Fig. 6).

In cyclohexylidene derivatives, substitution at C2 phenyl resulted in partial rotation of the molecules along C2-NH bond and hence a complete enclosure of hydrophobic groups in the binding pocket consequent to which all C2 phenyl substituted derivatives had higher binding energy than the core compound **3a** (Fig. 7).

Fig. 6 **a** 2D interaction diagram of **2a** in the active site of 3LAU **b** Hydrophobic enclosure of **2a** (red) and molecules with substituted C2 phenyl groups (blue) (color figure online)

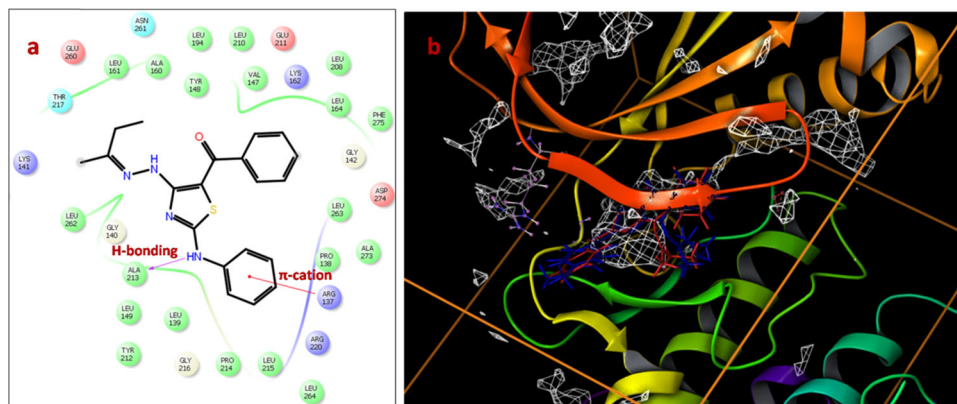


Fig. 7 **a** Hydrophobic enclosure of **3a** in the active site of 3LAU **b** Hydrophobic enclosure of molecules with substituted C2 phenyl groups

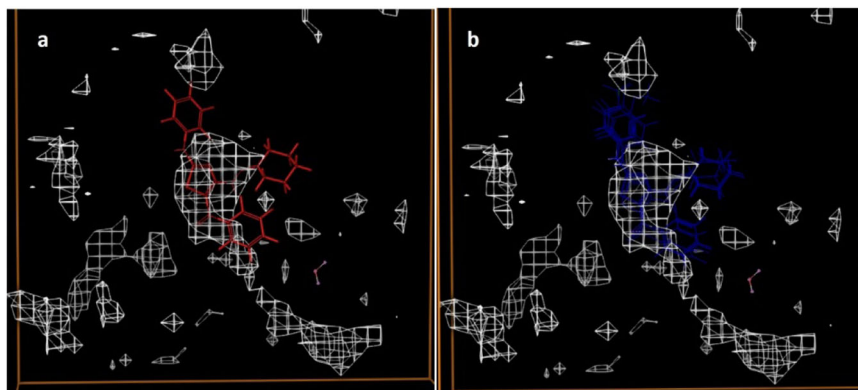
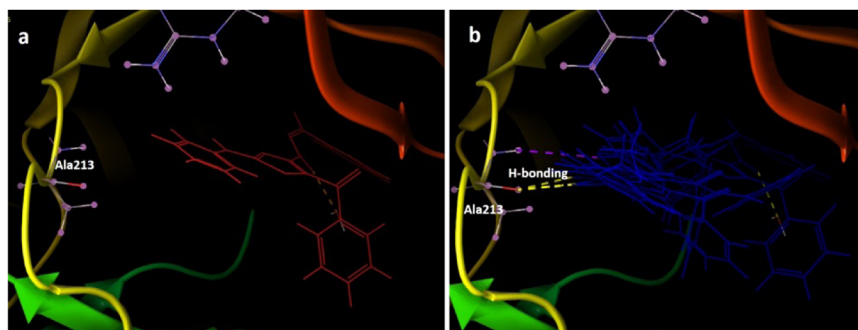


Fig. 8 **3D** binding mode of **a 4a** and **b** molecules with substituted C2 phenyl groups in the active site of 3LAU protein



In BzHAT class, core molecule **4a** bound to the active site away from hinge region without any H-bonding interactions with binding pocket. The R₃ substitution was found to have significant effect on locating hydrophobic rings in protein binding site which increased binding affinity toward protein through H-bonding with Ala213 (Fig. 8).

It was found that in all four classes, R₃ substitution was desirable for better interaction with hinge region and thereby increased binding energy than corresponding unsubstituted analogs.

Effect of R₄ substitution

The docking studies on HAT derivatives with substituted phenyl rings at R₄ revealed that in all classes –NO₂/–OMe substitutions increase binding affinity by reducing exposure penalty effected through an orientation change in the active site (Fig. 9). However, halogen substitutions were not much influential in modulating the binding affinity of the molecules in the 3LAU active site.

The replacement of phenyl ring at C5 with a poly aromatic ring such as naphthalene increased the binding energy of IPHAT, IBHAT, and CyHAT whereas in BzHAT bind-

ing affinity was significantly reduced. This decrease was attributed to solvent exposure of hydrophobic rings. Furthermore, modification of R₄ with biologically relevant heterocyclic ring systems such as coumarin and indole led to enhanced binding energies wherein a more pronounced effect was found for indolyl derivatives (Table 6). The in silico screening in protein active site clearly indicated a substantial effect of binding pattern of the molecules with change in the substitution around the core which can be utilized for hit to lead identification in a structure-based drug design (SBDD) protocol.

Fig. 9 Binding orientations of **a** **1a** and and F-substituted molecule in 3LAU active site **b** Binding orientations of –OMe and –NO₂ substituted molecules in 3LAU active site

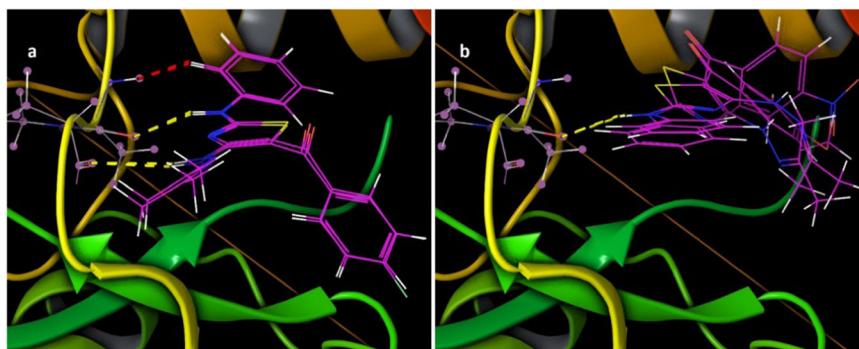


Table 6 Binding energy of HAT with poly/heteroaromatic R₄

R ₃	R ₄	GScore, LiophilicEvdW, Hbond, Electro			
		IPHAT	IBHAT	CyHAT	BzHAT
		–4.69	–6.56	–6.05	–5.09
		–5.14	–3.87	–4.19	–3.9
		0	–0.7	–0.7	–0.65
		–0.08	–0.14	–0.19	–0.41
		–7.80	–6.34	–6.35	–5.41
		–5.50	–3.94	–5.63	–5.07
		–1.33	–0.7	–1.18	–0.7
		–0.39	–0.29	–0.25	–0.25
		–8.90	–7.17	–6.41	–6.82
		–4.91	–4.86	–4.79	–4.53
		–1.83	–0.7	–0.7	–1.11
		–0.46	0.02	0.06	–0.34
		–6.98	–6.89	–7.27	–6.75
		–4.48	–3.93	–4.25	–4.48
		–1.01	–1.11	–1.05	–0.7
		–0.33	–0.49	–0.37	–0.2

Conclusion

A novel tetravariant scaffold based on 2-aminothiazole template, viz; 4-hydrazinotiazoles (HAT), was designed for small molecule drug design. The immense scope for enriching biologically relevant chemical space through diversity multiplication around the core was envisaged by the synthesis of twelve derivatives through [4 + 1] ring closure. The anticancer activity of the compounds in six human cancer cell lines had identified two structural analogs of DAT1 (**2b**, **4b**) to be active against MCF-7 and one against (**3b**) A549 cancer cell lines. The in silico ADME prediction showed the drug-likeness of the molecules and the virtual screening in three classes of anticancer target proteins showed significant affinity towards Aurora kinase protein suggesting possibility of the scaffold to be developed as Aurora inhibitors. Thus a VCHATL of 200 molecules was designed and molecular docking studies performed in the selected Aurora kinase proteins revealed an ATP competitive mode which further indicated the scope of the scaffold to be developed as a new class of Aurora kinase inhibitors.

Acknowledgements ST acknowledges IIST for financial support. Thanks are due to NIIST-TVM, IISER-TVM for support in NMR recording and ACTREC Mumbai for in vitro anticancer screening.

Compliance with ethical standards

Conflict of interest The authors declare that they have no competing interests.

References

- Altıntop MD, Özdemir A, Turan-Zitouni G, Ilgin S, Atlı Ö, Demirci F, Kaplancıklı ZA (2014) Synthesis and in vitro evaluation of new nitro-substituted thiazolyl hydrazone derivatives as anticandidal and anticancer agents. *Molecules* 19:14809–14820
- Ayati A, Emami S, Asadipour A, Shafiee A, Foroumadi A (2015) Recent applications of 1, 3-thiazole core structure in the identification of new lead compounds and drug discovery. *Eur J Med Chem* 97:699–718
- Bennani YL (2012) Drug discovery in the next decade: innovation needed ASAP. *Drug Discov Today* 17:S31–S44
- Bharti SK, Nath G, Tilak R, Singh S (2010) Synthesis, anti-bacterial and anti-fungal activities of some novel Schiff bases containing 2, 4-disubstituted thiazole ring. *Eur J Med Chem* 45:651–660
- Carpinelli P, Ceruti R, Giorgini ML, Cappella P, Gianellini L, Croci V, Degrossi A, Texido G, Rocchetti M, Vianello P (2007) PHA-739358, a potent inhibitor of Aurora kinases with a selective target inhibition profile relevant to cancer. *Mol Cancer Ther* 6:3158–3168
- Carradori S, Secci D, Bolasco A, Rivanera D, Mari E, Zicari A, Lotti LV, Bizzarri B (2013) Synthesis and cytotoxicity of novel (thiazol-2-yl) hydrazine derivatives as promising anti-Candida agents. *Eur J Med Chem* 65:102–111
- Chen G, Zheng S, Luo X, Shen J, Zhu W, Liu H, Gui C, Zhang J, Zheng M, Puaah CM (2005) Focused combinatorial library design based on structural diversity, druglikeness and binding affinity score. *J Comb Chem* 7:398–406
- Cheng Y, Avula SR, Gao W-W, Addla D, Tanganchu VKR, Zhang L, Lin J-M, Zhou C-H (2016) Multi-targeting exploration of new 2-aminothiazolyl quinolones: synthesis, antimicrobial evaluation, interaction with DNA, combination with topoisomerase IV and penetrability into cells. *Eur J Med Chem* 124:935–945
- Dandawate P, Ahmad A, Deshpande J, Swamy KV, Khan EM, Khetmalas M, Padhye S, Sarkar F (2014) Anticancer phytochemical analogs 37: synthesis, characterization, molecular docking and cytotoxicity of novel plumbagin hydrazones against breast cancer cells. *Bioorg Med Chem Lett* 24:2900–2904
- Das D, Sikdar P, Bairagi M (2016) Recent developments of 2-aminothiazoles in medicinal chemistry. *Eur J Med Chem* 109:89–98
- Deng Z-L, Du C-X, Li X, Hu B, Kuang Z-K, Wang R, Feng S-Y, Zhang H-Y, Kong D-X (2013) Exploring the biologically relevant chemical space for drug discovery. *J Chem Inf Model* 53:2820–2828
- Dilek Altıntop M, Cantürk Z, Baysal M, Asım Kaplancıklı Z (2016) Synthesis and evaluation of new thiazole derivatives as potential antimicrobial agents. *Lett Drug Des Discov* 13:903–911
- Dilek Altıntop M, Özdemir A, Ilgin S, Atlı O (2014) Synthesis and biological evaluation of new pyrazole-based thiazolyl hydrazone derivatives as potential anticancer agents. *Lett Drug Des Discov* 11:833–839
- Dimova D, Bajorath J (2016) Systematic design of analogs of active compounds covering more than 1000 targets. *MedChemComm* 7:859–863
- Dobson CM (2004) Chemical space and biology. *Nature* 432:824–828
- Dua R, Shrivastava S, Sonwane S, Srivastava S (2011) Pharmacological significance of synthetic heterocycles scaffold: a review. *Adv Biol Res* 5:120–144
- Fancelli D, Moll J, Varasi M, Bravo R, Artico R, Berta D, Bindi S, Cameron A, Candiani I, Cappella P (2006) 1, 4, 5, 6-tetrahydropyrrolo [3, 4-c] pyrazoles: identification of a potent Aurora kinase inhibitor with a favorable antitumor kinase inhibition profile. *J Med Chem* 49:7247–7251
- Friesner RA, Murphy RB, Repasky MP, Frye LL, Greenwood JR, Halgren TA, Sanschagrin PC, Mainz DT (2006) Extra precision glide: docking and scoring incorporating a model of hydrophobic enclosure for protein-ligand complexes. *J Med Chem* 49:6177–6196
- Gallardo-Godoy A, Gever J, Fife KL, Silber BM, Prusiner SB, Renslo AR (2011) 2-Aminothiazoles as therapeutic leads for prion diseases. *J Med Chem* 54:1010–1021
- Gorczynski MJ, Leal RM, Mooberry SL, Bushweller JH, Brown ML (2004) Synthesis and evaluation of substituted 4-aryloxy-and 4-arylsulfanyl-phenyl-2-aminothiazoles as inhibitors of human breast cancer cell proliferation. *Bioorg Med Chem* 12:1029–1036
- Gorse A-D (2006) Diversity in medicinal chemistry space. *Curr Top Med Chem* 6:3–18
- Green DA, Antholine WE, Wong SJ, Richardson DR, Chitambar CR (2001) Inhibition of malignant cell growth by 311, a Novel Iron chelator of the pyridoxal isonicotinoyl hydrazone class effect on the R2 subunit of ribonucleotide reductase. *Clin Cancer Res* 7:3574–3579
- Hajduk PJ, Galloway WR, Spring DR (2011) Drug discovery: a question of library design. *Nature* 470:42–43
- Holla BS, Malini K, Rao BS, Sarojini B, Kumari NS (2003) Synthesis of some new 2, 4-disubstituted thiazoles as possible antibacterial and anti-inflammatory agents. *Eur J Med Chem* 38:313–318

- John Harris C, Hill RD, Sheppard DW, Slater MJ, Stouten PFW (2011) The design and application of target-focused compound libraries. *Comb Chem High Throughput Screen* 14:521–531
- Jorgensen WL, Maxwell DS, Tirado-Rives J (1996) Development and testing of the OPLS All-Atom force field on conformational energetics and properties of organic liquids. *J Am Chem Soc* 118:11225–11236
- Kalinowski DS, Sharpe PC, Bernhardt PV, Richardson DR (2007) Design, synthesis, and characterization of new iron chelators with anti-proliferative activity: structure-activity relationships of novel thiohydrazone analogs. *J Med Chem* 50:6212–6225
- Kaplánek R, Havlík M, Dolenský B, Rak J, Džubák P, Konečný P, Hajdúch M, Králová J, Král V (2015a) Synthesis and biological activity evaluation of hydrazone derivatives based on a Tröger's base skeleton. *Bioorg Med Chem* 23:1651–1659
- Kaplánek R, Jakubek M, Rak J, Kejk Z, Havlík M, Dolenský B, Frydrych I, Hajdúch M, Kolář M, Bogdanová K (2015b) Caffeine-hydrazones as anticancer agents with pronounced selectivity toward T-lymphoblastic leukemia cells. *Bioorg Chem* 60:19–29
- Kashyap SJ, Garg VK, Sharma PK, Kumar N, Dudhe R, Gupta JK (2012) Thiazoles: having diverse biological activities. *Med Chem Res* 21:2123–2132
- Lipinski C, Hopkins A (2004) Navigating chemical space for biology and medicine. *Nature* 432:855–861
- Lovejoy DB, Richardson DR (2002) Novel "hybrid" iron chelators derived from aroylhydrazones and thiosemicarbazones demonstrate selective antiproliferative activity against tumor cells. *Blood* 100:666–676
- Manfredi MG, Ecsedy JA, Meetze KA, Balani SK, Burenkova O, Chen W, Galvin KM, Hoar KM, Huck JJ, LeRoy PJ (2007) Antitumor activity of MLN8054, an orally active small-molecule inhibitor of Aurora A kinase. *Proc Natl Acad Sci* 104:4106–4111
- Mortlock AA, Foote KM, Heron NM, Jung FH, Pasquet G, Lohmann J-JM, Warin N, Renaud F, De Savi C, Roberts NJ (2007) Discovery, synthesis, and in vivo activity of a new class of pyrazoloquinazolines as selective inhibitors of aurora B kinase. *J Med Chem* 50:2213–2224
- Nasr T, Bondock S, Youns M (2014) Anticancer activity of new coumarin substituted hydrazide-hydrazone derivatives. *Eur J Med Chem* 76:539–548
- Novinson T, Bhooshan B, Okabe T, Revankar GR, Robins RK, Senga K, Wilson HR (1976) Novel heterocyclic nitrofurural hydrazones. In vivo antitrypanosomal activity. *J Med Chem* 19:512–516
- Paula SSP, Yardilyb A, Rajasekharan K, Reji TAF (2013) Synthesis of anticancer compounds 2-(4-amino-2-arylaminothiazol-5-yl)-N-methylbenzimidazoles. *Indian J Chem* 52:560–564
- Prien O (2005) Target-family-oriented focused libraries for kinases—conceptual design aspects and commercial availability. *Chem-BioChem* 6:500–505
- Rodrigues T, Reker D, Welin M, Caldera M, Brunner C, Gabernet G, Schneider P, Walse B, Schneider G (2015) De Novo fragment design for drug discovery and chemical biology. *Angew Chem Int Ed* 54:15079–15083
- Rollas S, Küçükgülzel SG (2007) Biological activities of hydrazone derivatives. *Molecules* 12:1910–1939
- Romagnoli R, Baraldi PG, Carrion MD, Cruz-Lopez O, Lopez Cara C, Basso G, Viola G, Khedr M, Balzarini J, Mahboobi S (2009) 2-Arylamino-4-amino-5-aryloxythiazoles. "One-pot" synthesis and biological evaluation of a new class of inhibitors of tubulin polymerization. *J Med Chem* 52:5551–5555
- Savini L, Chiasserini L, Travagli V, Pellerano C, Novellino E, Cosentino S, Pisano MB (2004) New α -(N)-heterocyclhydrazones: evaluation of anticancer, anti-HIV and antimicrobial activity. *Eur J Med Chem* 39:113–122
- Schneider G, Fechner U (2005) Computer-based de novo design of drug-like molecules. *Nat Rev Drug Discov* 4:649–663
- Schneider G, Schneider P (2016) Coping with complexity in ligand-based de novo design. *Frontiers in molecular design and chemical information Science—Herman Skolnik Award Symposium 2015: Jürgen Bajorath*. ACS Publications
- Schrödinger (2014) Maestro, version 9.6. LLC, New York, NY
- Secci D, Bizzarri B, Bolasco A, Carradori S, D'Ascenzio M, Rivanera D, Mari E, Polletta L, Zicari A (2012) Synthesis, anti-Candida activity, and cytotoxicity of new (4-(4-iodophenyl) thiazol-2-yl) hydrazine derivatives. *Eur J Med Chem* 53:246–253
- Sengupta S, Smitha SL, Thomas NE, Santhoshkumar TR, Devi SK, Sreejalekshmi KG, Rajasekharan KN (2005) 4-Amino-5-benzoyl-2-(4-methoxyphenylamino) thiazole (DAT1): a cytotoxic agent towards cancer cells and a probe for tubulin-microtubule system. *Br J Pharmacol* 145:1076–1083
- Sheppard DW, MacRitchie JA (2013) Building in molecular diversity for targeted libraries. *Drug Discov Today* 10:e461–e466
- Skehan P, Storeng R, Scudiero D, Monks A, McMahon J, Vistica D, Warren JT, Bokesch H, Kenney S, Boyd MR (1990) New colorimetric cytotoxicity assay for anticancer-drug screening. *J Natl Cancer Inst* 82:1107–1112
- Song Y, Chen W, Kang D, Zhang Q, Zhan P, Liu X (2014) "Old friends in new guise": exploiting privileged structures for scaffold re-evolution/refining. *Comb Chem High Throughput Screen* 17:536–553
- Sreejalekshmi K (2010) A facile, sequential multicomponent approach to N-aminoamidinothioureas—versatile syntheses to bioactive heterocycles. *Phosphorus Sulfur Silicon* 185:1830–1837
- Tian F-F, Jiang F-L, Han X-L, Xiang C, Ge Y-S, Li J-H, Zhang Y, Li R, Ding X-L, Liu Y (2010) Synthesis of a novel hydrazone derivative and biophysical studies of its interactions with bovine serum albumin by spectroscopic, electrochemical, and molecular docking methods. *J Phys Chem B* 114:14842–14853
- Titus S, Sreejalekshmi KG (2014) One-pot four-component synthesis of 4-hydrazinothiazoles: novel scaffolds for drug discovery. *Tetrahedron Lett* 55:5465–5467
- Urich R, Wishart G, Kiczun M, Richters A, Tidten-Luksch N, Rauh D, Sherborne B, Wyatt PG, Brenk R (2013) De novo design of protein kinase inhibitors by in silico identification of hinge region-binding fragments. *ACS Chem Biol* 8:1044–1052
- Verma G, Marella A, Shaquiquzzaman B, Akhtar M, Ali MR, Alam MM (2014) A review exploring biological activities of hydrazones. *J Pharm Bioallied Sci* 6:69
- Vichai V, Kirtikara K (2006) Sulforhodamine B colorimetric assay for cytotoxicity screening. *Nat Protoc* 1:1112–1116
- Welsch ME, Snyder SA, Stockwell BR (2010) Privileged scaffolds for library design and drug discovery. *Curr Opin Chem Biol* 14:347–361
- Wilkinson RW, Odedra R, Heaton SP, Wedge SR, Keen NJ, Crafter C, Foster JR, Brady MC, Bigley A, Brown E (2007) AZD1152, a selective inhibitor of Aurora B kinase, inhibits human tumor xenograft growth by inducing apoptosis. *Clin Cancer Res* 13:3682–3688
- Yan A, Wang L, Xu S, Xu J (2011) Aurora-A kinase inhibitor scaffolds and binding modes. *Drug Discov Today* 16:260–269
- Yu X, Shi L, Ke S (2015) Acylhydrazone derivatives as potential anticancer agents: synthesis, bio-evaluation and mechanism of action. *Bioorg Med Chem Lett* 25:5772–5776
- Yurtaş L, Özkay Y, Kaplancıklı ZA, Tunalı Y, Karaca H (2013) Synthesis and antimicrobial activity of some new hydrazone-bridged thiazole-pyrrole derivatives. *J Enzyme Inhib Med Chem* 28:830–835